Density Functional Theory Calculations of Solid Nitromethane under Hydrostatic and Uniaxial Compressions with Empirical van der Waals Correction

M. W. Conroy,*,† I. I. Oleynik,† S. V. Zybin,‡ and C. T. White§

Department of Physics, University of South Florida, Tampa, Florida 33620, Materials and Process Simulation Center, California Institute of Technology, Pasadena, California 91125, and Naval Research Laboratory, Washington, DC 20375

Received: November 7, 2008; Revised Manuscript Received: February 16, 2009

First-principles density functional theory calculations have been performed with and without an empirical van der Waals (vdW) correction to obtain constitutive relationships of solid nitromethane under hydrostatic and uniaxial compressions. The unit-cell parameters at zero pressure and the hydrostatic equation of state at 0 K are in reasonable agreement with experimental data using pure DFT, and the agreement is significantly improved with the inclusion of the vdW dispersion correction. Uniaxial compressions normal to the {100}, {010}, {001}, {110}, {101}, {011}, and {111} planes were performed, and a comparison of the principal stresses, changes in energy, and shear stresses for different compression directions clearly indicate anisotropic behavior of solid nitromethane upon compression. The calculated anisotropic constitutive relationships might help to link the anisotropic shock sensitivity and the underlying atomic-scale properties of solid nitromethane.

I. Introduction

Nitromethane (NM) is a generic explosive material which, because of its relatively simple molecular structure, is widely used in experimental studies of fundamental properties of energetic materials. With the simplicity of the NM molecule, CH_3NO_2, and the small size of the unit cell of NM molecular crystal (Figure 1), the implementation of theoretical methods and the understanding of experimental results is greatly facilitated. Because the microscopic mechanisms leading to detonation have yet to be fully understood, it is advantageous to study such a simple material in an effort to elucidate its physical behavior at the onset of shock-induced detonation.

At ambient conditions, nitromethane is a liquid, yet it is found to be in a solid at low temperatures[1] as well as at room temperature for pressures as low as 0.3 GPa.[2] The structure of solid nitromethane was determined by Trevino et al.[1] using a combination of X-ray and neutron diffraction: the solid NM possesses an orthorhombic $P2_12_12_1$ space group and lattice constants $a = 5.183$ Å, $b = 6.235$ Å, and $c = 8.518$ Å at 4.2 K.

Hydrostatic compression experiments have been performed by Cromer et al.,[2] Yarger and Olinger,[3] and Citroni et al.[4] Cromer et al. used X-ray diffraction to study compression of single-crystal NM in a diamond-anvil cell (DAC) at room temperature and pressures between 0.3 and 6.0 GPa. Yarger and Olinger[3] also performed X-ray diffraction experiments of the hydrostatic compression of solid nitromethane up to 15 GPa. Citroni et al.[4] extended the pressure up to 27.3 GPa, near the detonation threshold, using a DAC and angle dispersion X-ray diffraction. The data from these studies[2−4] indicate that nitromethane maintains its $P2_12_12_1$ space group up to 27.3 GPa. However, Courtecuisse et al.[5] reported four solid phase transitions of nitromethane at approximately 3, 7.5, 13.2, and 25 GPa observed in DAC experiments performed at ambient temperature. More recent studies[4,6] claim that the phase transitions[5] reported by Courtecuisse et al. are changes in the molecular structure that do not change the crystal symmetry.

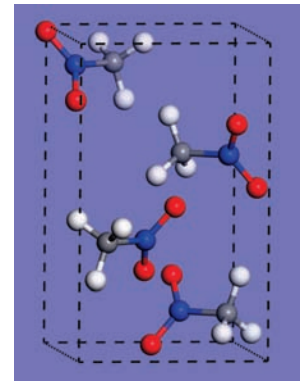

Figure 1. Unit cell of solid nitromethane.

DAC compression experiments have also been performed by Piermarini et al.[7] They found that explosions were observed when solid nitromethane was compressed with either the {011} or the {110} crystal faces parallel to the anvil faces. This anisotropic effect was not observed with deuterated nitromethane.[7]

Theoretical investigations into the sensitivity of solid nitromethane have been performed by Dick[8] who developed a model based upon steric hindrance to shear to predict anisotropic sensitivity. His results indicate that compression in the <100> direction would be a direction of greater sensitivity under the assumptions of his model.[8] The lack of the greater sensitivity for the directions reported by Peirmarini et al.[7] was explained by Dick as the absence of the uniaxial strain in the DAC compression experiments.[8] Reed et al.[9] have performed density-functional theory (DFT) molecular dynamics (MD) simulations of NM to examine the possible role of the electronic excitations in shock-induced initiation.[10−14] Their simulations indicate that static compressions do not significantly lower the band gap.

† University of South Florida.
‡ California Institute of Technology.
§ Naval Research Laboratory.

10.1021/jp809843k CCC: $40.75
Published on Web 03/25/2009

TABLE 1: Calculated Zero-Pressure Lattice Constants and Volume of Solid Nitromethane Compared with Experimental Data

work	a (Å)	b (Å)	c (Å)	V (Å^3)
Trevino et al.[1]	5.183	6.236	8.518	275.3
this work: DFT without vdW correction	5.301 (+2.3%)	6.591 (+5.7%)	8.838 (+3.8%)	308.8 (+12%)
this work: DFT with vdW correction	5.176 (−0.1%)	6.274 (+0.6%)	8.537 (+0.2%)	277.3 (+0.7%)

However, their recent density-functional-based tight-binding molecular dynamics simulations of shock-compressed NM indicate that it forms a transient quasimetallic layer near the shock wave front.[15]

The mechanical properties of NM have also been investigated by theoretical methods. Byrd et al.[16] examined the limitations of DFT calculations in predicting equilibrium structures for energetic materials including nitromethane. It was suggested that DFT calculations lack the proper description of van der Waals (vdW) forces which results in overestimation of unit-cell volume for molecular crystals.[16,17] Liu et al.[18] used DFT to perform calculations of hydrostatic compression and the resulting vibrational spectra of solid nitromethane up to 20 GPa. Zerilli et al.[19] used both Hartree−Fock and DFT calculations to study the properties of solid nitromethane including its band structure. In addition to first-principles calculations, classical interatomic potential MD simulations have been performed by Sorescu et al.[20] using a Buckingham potential with added electrostatic interactions. They predicted the structural properties of the NM crystal in good agreement with experiment.

Several groups have worked to improve the description of vdW interactions within DFT for closed-shell systems such as NM. While some researchers[21−24] make first-principles approximations in the exchange-correlation functionals within DFT to describe nonlocal dispersion interactions, others[25−28] have taken an empirical approach by introducing pair potentials with the asymptotic C_6r^{-6} behavior. We have recently added an empirical vdW correction to DFT calculations[29] that is based on the work of Neumann and Perrin,[28] and it was used in the calculations of this study.

The major goals of this work are to evaluate the agreement of vdW-corrected DFT results with experimental data for solid NM and to examine its anisotropic response by performing uniaxial compressions in several low-index crystallographic directions using vdW-corrected DFT calculations. As mentioned above, previous DAC experiments indicate anisotropic sensitivity of this crystal under compression.[7,8] Therefore, an extension of the isotropic equation of state (EOS) to include the mechanical response to uniaxial compression might help identify physical factors that are responsible for the observed anisotropy. In particular, we are interested in the shear stresses upon compression because they are the major stimuli of plastic deformations in solids which might lead to mechanically induced chemical reactions in molecular crystals at shock wave conditions.

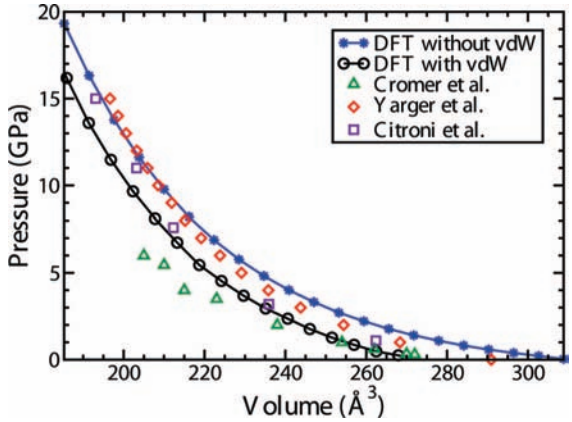

Figure 2. Isothermal hydrostatic EOS of solid nitromethane. The interval of volume shown is from 60% to 100% of the calculated zero-pressure volume.

II. Computational Details

The Vienna ab initio simulation package (VASP) code[30,31] was used to perform first-principles density-functional theory[32,33] (DFT) calculations of hydrostatic and uniaxial compressions of solid nitromethane. In previous work,[42] tests were performed to determine the exchange-correlation functional, pseudopotential, kinetic energy cutoff, and k-point sampling to obtain sufficiently accurate results for pure DFT calculations. The PBE functional[34,35] and the PAW potential[36,37] were chosen for pure DFT because this combination yielded better agreement with the experimental structure at equilibrium than any other combination involving the PW91 functional[38,39] and/or ultrasoft pseudopotentials.[40,41] The PW91 functional with the PAW potential was used for vdW-corrected DFT calculations because the empirical parameters for the model[28] were fitted using results obtained in this manner. An energy cutoff of 700 eV for both the pure DFT and vdW-corrected DFT calculations was used, and this resulted in convergence of the energy per atom to within 0.002 eV of calculations performed with an extremely large basis set corresponding to energy cutoff of 2 keV. The k-point sets used for each compression were determined by finding the set of k-points that corresponded to a spacing of 0.08 A^{-1} when the volume of the unit cell was scaled by 50% in a manner consistent with the given compression. With this method of obtaining the k-points for the calculations, the energy per atom at equilibrium was converged to within approximately 10^{-5} eV as compared to the results of a more accurate calculation with a 4 × 4 × 4 MP grid (32 k-points).

The relaxations for DFT without the vdW correction were performed using the quasi-Newton relaxation algorithm as implemented in VASP with the tolerance for convergence of electronic energies set to 10^{-6} eV. It was later found that the conjugate-gradient relaxation method within VASP reduced the cost of the calculations and reduced the difficulty in relaxing the structures at high compression to the desired tolerance for the maximum force on an atom in the unit cell, 0.03 eV/Å. Hence, this technique was used for all DFT calculations with the vdW correction.

The initial unit cell, built using experimental data by Trevino et al.,[1] was relaxed to determine the theoretical zero-pressure structure. The relaxation was performed without constraining the cell volume, cell shape, or the atomic coordinates. For the hydrostatic-compression simulation, the unit cell was compressed from 100% to 60% of its calculated zero-pressure volume, V_0, in increments of 2%. After scaling of the lattice constants and atomic coordinates, the unit cell was relaxed under the constraint of constant volume without a restraint on cell shape or atomic coordinates. For the uniaxial-compression simulations, the unit cell was compressed along seven low-index crystallographic directions, <100>, <010>, <001>, <110>, <101>, <011>, and <111>, from 100% to 70% of its zero-

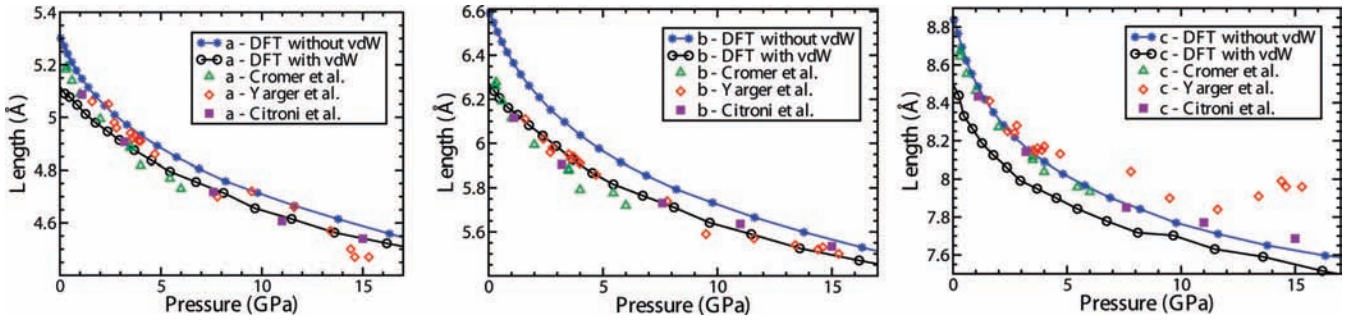

Figure 3. Lattice parameters of solid nitromethane under hydrostatic compression.

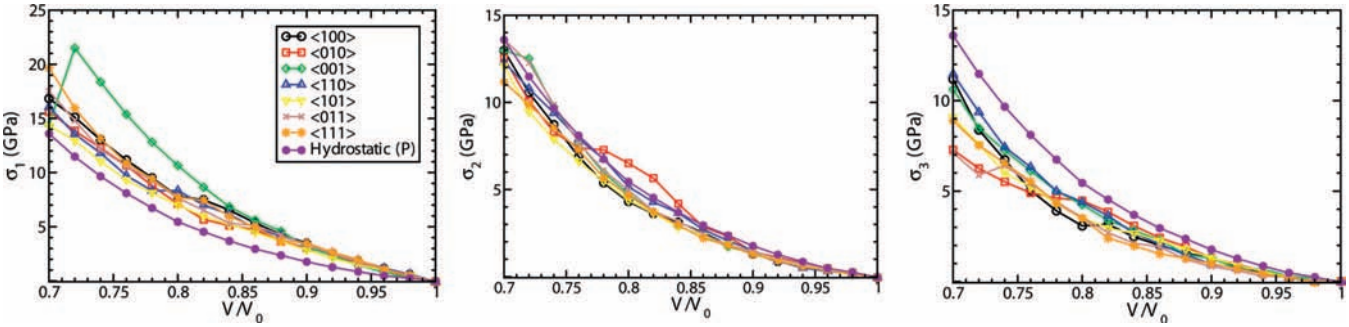

Figure 4. Principal stresses as a function of V/V_0 calculated with vdW correction. The pressure from the hydrostatic-compression calculations is shown for comparison.

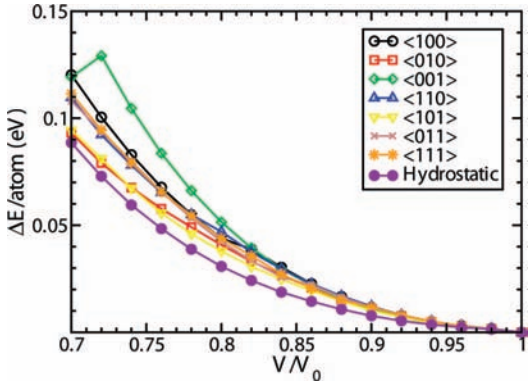

Figure 5. Change in energy upon uniaxial compression as a function of V/V_0 calculated with vdW correction.

pressure volume V_0 in increments of 2%. The uniaxial compressions were performed by aligning the desired compression direction with the x axis, scaling the x components of each lattice vector, and then relaxing the atomic coordinates within a fixed unit cell.

III. Equilibrium Properties and Hydrostatic EOS

The lattice constants and volume of the calculated zero-pressure structure of solid nitromethane are compared with the experimental data of Trevino et al.[1] in Table 1. The percent error for the lattice constants using DFT alone is approximately 2−6%, which is slightly greater than the error in our calculations of the zero-pressure structure of PETN,[42] HMX,[43] and RDX.[44] The vdW-corrected calculations significantly improve the agreement with experiment, reducing the error in the lattice parameters and unit-cell volume to less than 1% each.

The isothermal EOS calculated from the hydrostatic-compression simulation is compared with the experimental data of Yarger and Olinger,[3] Cromer et al.,[2] and Citroni et al.[4] in Figure 2. At low pressures, the vdW-corrected data shows better agreement with the data of Cromer et al. and Citroni et al., but there does not appear to be an improvement in the agreement with the data of Yarger and Olinger. As observed in similar work by Liu et al.,[18] the agreement between the hydrostatic-compression data by DFT alone and experiment increases at high pressure. Above 10 GPa, the pure DFT calculations show very good agreement with the data of Yarger et al. and Citroni et al.

The calculated lattice constants as functions of pressure are also compared with the experimental data[2−4] for hydrostatic compression in Figure 3. The lattice constant b appears to show better agreement with experiment when calculated with the vdW correction, while the pure-DFT results show better agreement for c. There are mixed results in the agreement of calculated results with experimental data of Yarger and Olinger and Cromer et al. for the a lattice constant, but the vdW-corrected DFT results show very good agreement with the more recent result of Citroni et al. Also, it appears that the experimental data of Yarger and Olinger for the a and c lattice constants begin to differ from our calculations above 13 GPa.

We also calculated the bulk modulus of NM (see Table 2). To be consistent with the bulk-modulus values reported in experimental studies, the calculated hydrostatic-compression data up to about 15 GPa were fit to the Murnaghan EOS

$$P = \frac{B_0}{B'_0}\left[\left(\frac{V}{V_0}\right)^{B'_0} - 1\right] \quad (1)$$

where B_0 is the bulk modulus at zero pressure, B'_0 is a derivative with respect to pressure, and V_0 is the unit-cell volume at zero pressure. Our pure-DFT results for both B_0 and B'_0 are in good agreement with the values reported by Cromer et al.[2] and Citroni et al.,[4] which were also fit to the Murnaghan EOS. The vdW-corrected calculations yield a larger value of B_0, but the agreement for B'_0 is similar to the value obtained with pure DFT.

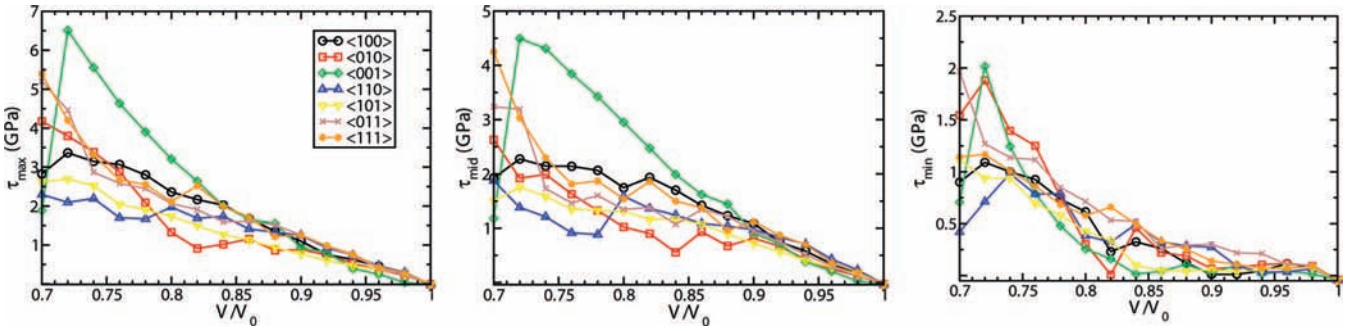

Figure 6. Shear stresses calculated with vdW correction.

TABLE 2: Bulk Modulus and Its Derivative with Respect to Pressure

source	experiment/theory	B_0 (GPa)	B'_0
Cromer et al. (ref 2)	experiment (Murnaghan)	7.0	5.7
Yarger and Olinger (ref 3)	experiment (reported)	10.1	–
Citroni et al. (ref 4)	experiment (Murnaghan)	8.3	5.9
this work: DFT without vdW correction	theory (Murnaghan)	8.0	5.1
this work: DFT with vdW correction	theory (Murnaghan)	12.9	5.3

IV. Uniaxial Compressions

The calculated principal stresses, i.e., eigenvalues of the stress tensor, for each uniaxial compression as a function of compression ratio V/V_0 using the vdW correction are shown in Figure 4. The principal stresses have been arranged such that σ_1 is the maximum and σ_3 is the minimum. Note that x is the direction of compression and σ_1 is approximately equal to σ_{xx} of the stress tensor. The calculated maximum principal stress σ_1 displays the anisotropic character of the constitutive properties of solid nitromethane. For compression up to about $V/V_0 = 0.88$, the similar values of σ_1 for each direction indicate isotropic behavior in this compression regime. However, at higher compression, the <001> compression clearly shows the greatest value of σ_1. The DFT calculations performed by Reed et al.[9] also indicated that compression in the <001> direction exhibited greater uniaxial stress than compression in the <100> and <010> directions.

The last data point at $V/V_0 = 0.70$ for the <001> compression shows a great reduction in the principal stresses as well as the energy and shear stresses, as shown in the figures below. From an observation of the structure of the unit cell during the relaxation, the NM molecules rotate, possibly to relieve the large stress in the unit cell. Our calculations show a change in symmetry of the crystal from $P2_12_12_1$ at $V/V_0 = 0.72$ to $P2_1$ at $V/V_0 = 0.70$.

The other principal stresses, σ_2 and σ_3, do not show a significant variation between different uniaxial compressions. Note that the pressure from the hydrostatic compression, identical to the principal stresses for this particular case, is also displayed in each graph for comparison.

Figure 5 shows the change in energy as a function of compression for each of the uniaxial compressions studied, and the hydrostatic-compression data is also included for comparison. Each of the directions are very similar up to about $V/V_0 = 0.84$, where the <001> compression begins to show the greatest change in energy. The <100>, <111>, and <110> directions display similar behavior, showing a greater change in energy per atom than two other directions with similar behavior, <101> and <010>. All uniaxial compressions raise the energy per atom more than hydrostatic compression.

V. Shear Stresses

Figure 6 exhibits the maximum shear stresses, τ_{max}, τ_{mid}, and τ_{min}, as a function of V/V_0 for each uniaxial compression. The principal stresses were used to calculate the maximum shear stresses via the equation

$$\tau = \frac{\sigma_i - \sigma_j}{2} \tag{2}$$

where $i \neq j$ take the values 1, 2, and 3. For each compression, the maximum shear stress τ_{max} is found by using $i = 1$ and $j = 3$. However, the ordering of i and j needed to calculate τ_{mid} and τ_{min} depends on the values of the principal stresses and must be chosen such that $\tau_{mid} \geq \tau_{min}$.

The calculated shear stresses τ_{max} and τ_{mid} as a function of V/V_0 also show anisotropic behavior. The <001> compression clearly shows the largest shear stress below $V/V_0 = 0.82$, and the shear stress has monotonic dependence on strain. Nonmonotonic dependence of shear stress on strain is observed in a small range of compression for the <010> and <110> compressions starting near $V/V_0 = 0.86$ and 0.80, respectively. This feature was also observed in the <100> direction of PETN,[42] which is found to be an insensitive direction in this material. The values of τ_{min} are small in comparison with τ_{max} and τ_{mid} and thus are assumed to be less significant as a source of plastic deformation.

Piermarini et al. reported explosions of solid nitromethane in their DAC experiments when samples were rapidly compressed up to 3 GPa in the <111> direction and either the <100> or the <001> direction.[7] While the <111> and <001> compressions of this study show relatively large values of the shear stresses τ_{max} and τ_{mid} at high compression, the <100> compression shear-stress values appear to be similar to the other directions of the study. If one assumes that relatively large shear-stress values from our calculations are correlated with greater sensitivity in nitromethane, then our calculations predict that purely uniaxial compression in the <111> and <001> directions would exhibit greater sensitivity. Our prediction of greater sensitivity in the <001> direction agrees with the work of Dick that is based upon a steric-hindrance model.[8] However, as discussed by Dick, the strain was not purely uniaxial, and the explosions reported were not entirely reproducible.[8]

VI. Conclusions

Density-functional theory (DFT) with an empirical vdW correction was used to calculate both hydrostatic and uniaxial compressions of solid nitromethane. With DFT alone, the lattice parameters of the zero-pressure structure were found to be within 2−6% of experimental values, while the vdW-corrected data was able to predict the lattice parameters and the unit-cell

volume within 1% of experiment. The calculated hydrostatic-compression EOS was in reasonable agreement with experimental results. The vdW-corrected data showed better agreement with experimental isotherms at low pressures, but the pure DFT data showed better agreement at higher pressure.

The uniaxial compression data were used to calculate the energy change per atom, principal stresses, and shear stresses as functions of V/V_0 for compressions in the <100>, <010>, <001>, <110>, <101>, <011>, and <111> directions. The calculated quantities indicate anisotropic behavior of solid nitromethane under compression. Anisotropic behavior in shear stresses has also been observed in calculations performed on pentaerythritol tetranitrate (PETN), where nonmonotonic dependence of shear stress upon strain coincides with directions that are insensitive to shock compression and larger shear stresses coincide with directions of greater sensitivity. Although it is difficult to identify the exact directions of greater sensitivity in solid nitromethane from explosions reported in DAC experiments by Piermarini et al.,[7] our prediction of greater sensitivity for the <001> direction based upon greater shear stress agrees with Dick's steric-hindrance model prediction.[8]

Acknowledgment. The work at USF was supported by the Office of Naval Research (ONR) through the Naval Research Laboratory (NRL) and partly by the Army Research Office through the MURI on Insensitive Munitions, DURIP, and the USF Center for Functional Integrative Materials. The work at Caltech was supported by the ONR, and ARO through the MURI on Insensitive Munitions. The work at NRL was supported by ONR both directly and through NRL. The computations were performed using NSF Teragrid computational facilities (Grant Nos. TG-DMR070018N and TG-MCA08X040).

References and Notes

(1) Trevino, S. F.; Prince, E.; Hubbard, C. R. *J. Chem. Phys.* **1980**, *73*, 2996.
(2) Cromer, D. T.; Ryan, R. R.; Schiferl, D. *J. Phys. Chem.* **1985**, *89*, 2315.
(3) Yarger, F. L.; Olinger, B. *J. Chem. Phys.* **1986**, *85*, 1534.
(4) Citroni, M.; Datchi, F.; Bini, R.; Di Varia, M.; Pruzan, P.; Canny, B.; Schettino, V. *J. Phys. Chem. B* **2008**, *112*, 1095.
(5) Courtecuisse, S.; Cansell, F.; Fabre, D.; Petitet, J.-P. *J. Chem. Phys.* **1995**, *102*, 968.
(6) Ouillon, R.; Pinan-Lucarre', J.-P.; Canny, B.; Pruzan, Ph.; Ranson, P. *J. Raman Spectrosc.* **2008**, *39*, 354.
(7) Piermarini, G. J.; Block, S.; Miller, P. J. *J. Phys. Chem.* **1989**, *93*, 457.
(8) Dick, J. J. *J. Phys. Chem.* **1993**, *97*, 6193.
(9) Reed, E. J.; Joannopoulos, J. D.; Fried, L. E. *Phys. Rev. B* **2000**, *62*, 16500.
(10) Williams, F. *Adv. Chem. Phys.* **1971**, *21*, 289.
(11) Dremin, A. N.; Klimenko, V. Y.; Davidoe, O. N.; Zoludeva, T. A. In The Ninth Symposium (International) on Detonation, OCNR, Arlington, VA, 1989.
(12) Sharma, J.; Beard, B. C.; Chaykovsky, M. *J. Phys. Chem.* **1991**, *95*, 1209.
(13) Gilman, J. J. *Philos. Mag. B* **1995**, *71*, 1957.
(14) Kuklja, M. M.; Kunz, A. B. *J. Appl. Phys.* **1999**, *86*, 4428.
(15) Reed, E. J.; Manaa, M. R.; Fried, L. E.; Glaesemann, K. R.; Joannopoulos, J. D. *Nat. Phys.* **2008**, *4*, 72.
(16) Byrd, E. F. C.; Scuseria, G. E.; Chabalowski, C. F. *J. Phys. Chem. B* **2004**, *108*, 13100.
(17) Byrd, E. F. C.; Rice, B. M. *J. Phys. Chem. C* **2007**, *111*, 2787.
(18) Liu, H.; Zhao, J.; Wei, D.; Gong, Z. *J. Chem. Phys.* **2006**, *124*, 124501.
(19) Zerilli, F. J.; Hooper, J. P.; Kuklja, M. M. *J. Chem. Phys.* **2007**, *126*, 114701.
(20) Sorescu, D. C.; Rice, B. M.; Thompson, D. L. *J. Phys. Chem. B* **2000**, *104*, 8406.
(21) Rapcewicz, K.; Ashcroft, N. W. *Phys. Rev. B* **1991**, *44*, 4032.
(22) Dobson, J. F. In *Topics in Condensed Matter Physics*; Das, M. P., Ed.; Nova: New York, 1994.
(23) Andersson, Y.; Langreth, D. C.; Lundqvist, B. I. *Phys. Rev. Lett.* **1996**, *76*, 102.
(24) Kohn, W.; Meir, Y.; Makarov, D. E. *Phys. Rev. Lett.* **1998**, *80*, 4153.
(25) Elstner, M.; Hobza, P.; Fraunheim, T.; Suhai, S.; Kaxiras, E. *J. Chem. Phys.* **2001**, *114*, 5149.
(26) Wu, Q.; Yang, W. *J. Chem. Phys.* **2002**, *116*, 515.
(27) Grimme, S. *J. Comput. Chem.* **2004**, *25*, 1463.
(28) Neumann, M. A.; Perrin, M.-A. *J. Phys. Chem. B* **2005**, *109*, 15531.
(29) Conroy, M. W.; Lin, Y.; Oleynik, I. I.; White, C. T. Submitted for publication.
(30) Kresse, G.; Furthmuller, J. *Phys. Rev. B* **1996**, *54*, 11169.
(31) Kresse, G.; Furthmuller, J. *Comput. Mater. Sci.* **1996**, *6*, 15.
(32) Hohenberg, P.; Kohn, W. *Phys. Rev.* **1964**, *136*, B864.
(33) Kohn, W.; Sham, L. J. *Phys. Rev.* **1965**, *140*, A1133.
(34) Perdew, J. P.; Burke, K.; Ernzerhof, M. *Phys. Rev. Lett.* **1996**, *77*, 3865.
(35) Perdew, J. P.; Burke, K.; Ernzerhof, M. *Phys. Rev. Lett.* **1997**, *78*, 1396.
(36) Blochl, P. E. *Phys. Rev. B* **1994**, *50*, 17953.
(37) Kresse, G.; Joubert, D. *Phys. Rev. B* **1999**, *59*, 1758.
(38) Perdew, J. P.; Chevary, J. A.; Vosko, S. H.; Jackson, K. A.; Pederson, M. R.; Singh, D. J.; Fiolhais, C. *Phys. Rev. B* **1992**, *46*, 6671.
(39) Perdew, J. P.; Chevary, J. A.; Vosko, S. H.; Jackson, K. A.; Pederson, M. R.; Singh, D. J.; Fiolhais, C. *Phys. Rev. B* **1993**, *48*, 4978.
(40) Vanderbilt, D. *Phys. Rev. B* **1990**, *41*, 7892.
(41) Kresse, G.; Hafner, J. *J. Phys.: Condens. Matter* **1994**, *6*, 8245.
(42) Conroy, M. W.; Oleynik, I. I.; Zybin, S. V.; White, C. T. *Phys. Rev. B* **2008**, *77*, 094107.
(43) Conroy, M. W.; Oleynik, I. I.; Zybin, S. V.; White, C. T. *J. Appl. Phys.* **2008**, *104*, 053506.
(44) Conroy, M. W.; Oleynik, I. I.; Zybin, S. V.; White, C. T. *J. Appl. Phys.* **2008**, *104*, 113501.

JP809843K